

Hao-yu Liao

Environmental Engineering Sciences, University of Florida, Gainesville, FL 32611 e-mail: haoyuliao@ufl.edu

Yuhao Chen

Industrial and Systems Engineering, University of Florida, Gainesville, FL 32611 e-mail: yuhaochen@ufl.edu

Boyi Hu

Assistant Professor Industrial and Systems Engineering, University of Florida, Gainesville, FL 32611 e-mail: boyihu@ise.ufl.edu

Sara Behdad¹

Associate Professor Environmental Engineering Sciences, University of Florida, Gainesville, FL 32611 e-mail: sarabehdad@ufl.edu

Optimization-Based Disassembly Sequence Planning Under Uncertainty for Human-Robot Collaboration

Disassembly is an essential step for remanufacturing end-of-life (EOL) products. Optimization of disassembly sequences and the utilization of robotic technology could alleviate the labor-intensive nature of dismantling operations. This study proposes an optimization framework for disassembly sequence planning under uncertainty considering humanrobot collaboration. The proposed framework combines three attributes: disassembly cost, safety, and complexity of disassembly, namely disassembleability, to identify the optimal disassembly path and allocate operations between human and robot. A multiattribute utility function is used to address uncertainty and make a tradeoff among multiple attributes. The disassembly time reflects the cost of disassembly which is assumed to be an uncertain parameter with a Beta distribution; the disassembleability evaluates the feasibility of conducting operations by robot; finally, the safety index ensures the protection of human workers in the work environment. An example of dismantling a desktop computer is used to show the application. The model identifies the optimal disassembly sequence with less disassembly cost, high disassembleability, and increased safety index while allocating disassembly operations among human and robot. A sensitivity analysis is conducted to show the model's performance when changing the disassembly cost for the robot. [DOI: 10.1115/1.4055901]

Keywords: disassembly sequence planning, optimization, uncertainty, remanufacturing, human-robot collaboration, electronic waste, design for disassembly, design for the environment

1 Introduction

Proper recovery of electronic waste (e-waste) has considerable environmental and economic advantages [1]. A recommended practice for e-waste reduction is to extend the product life cycle through reuse, remanufacture, or recovery of components [2]. Disassembly is an inevitable step for the proper recovery of components from end-of-life (EOL) devices. One question often facing remanufacturers is to identify the best sequence to dismantle a device. Determining the optimal disassembly sequence plan is a challenging decision due to the complexity of product design [3], the need for considering multiple objectives [4], and aligning disassembly objectives with other production planning strategies [5].

A considerable number of studies have been focused on optimizing disassembly sequences to lower the remanufacturing cost [6–8]. Different normative techniques have been developed to find the optimal disassembly sequence. To name a few studies, Tseng et al. [9] developed a flatworm algorithm to lower disassembly times by reducing disassembly direction and required tools. Fu et al. [10] proposed a stochastic bi-objective disassembly planning to maximize profit while minimizing energy consumption. Xia et al. [11] developed a 3D-based multi-objective collaborative disassembly sequence planning method by prioritizing disassembly levels for parts. Lee et al. [12] applied a fuzzy scoring procedure to measure disassembly factors before using a genetic algorithm to select the best sequence. Behdad and Thurston [6] used multi-attribute utility theory to determine the optimal disassembly

¹Corresponding author.

sequence considering multiple attributes of cost and probability of components damage during disassembly and reassembly. Tao et al. [5] used the disassembly precedence matrix and a Tabu search algorithm to compare different disassembly strategies considering disassembly time, energy consumption, and cost. Ilgin and Taşoğlu [4] combined simulation modeling and genetic algorithm to simultaneously decide the best disassembly sequence and the optimal number of EOL products to recover. Mircheski et al. [13] developed a 3D CAD-integrated software tool to analyze design alternatives in terms of design for disassembly. While the previous studies have investigated disassembly sequence planning, the number of studies considering robotic-assisted disassembly and human–robot collaboration is limited.

Human–robot collaboration in disassembly is becoming a popular topic in recent years. The labor-intensive and repetitive nature of disassembly tasks may lead to human musculoskeletal disorders [14]. Robots can handle monotonous repetitive or hazardous tasks more efficiently than humans [14,15]. Although robots provide higher efficiency, human workers are still needed in disassembly operations for handling tasks that are difficult and inflexible for robots [16].

Previous studies have considered human–robot collaboration when deciding on disassembly sequence planning. For example, Lee et al. [17] considered disassembly rules, disassembly cost, and the position between human worker and robot and used a receding horizon control technique for real-time disassembly planning. Xu et al. [16] applied a discrete bees algorithm to determine disassembly sequence planning by considering time, cost, and difficulty of disassembly. Parsa and Saadat [18] used a genetic algorithm to optimize sequence planning, considering cleanability, repairability, and economy. Xu et al. [19] adopted a multi-objective artificial bee colony algorithm and AND/OR graph to find the optimal disassembly sequence considering disassembly failure risks, disassembly

Contributed by the Design for Manufacturing Committee of ASME for publication in the JOURNAL OF MECHANICAL DESIGN. Manuscript received August 1, 2022; final manuscript received September 29, 2022; published online November 1, 2022. Assoc. Editor: Paul Witherell.

priority, cycle time, and cost. Li et al. [14] considered human fatigue to evaluate disassembly efficiency and used the bees algorithm to arrange tasks among humans and robots. Xu et al. [20] considered the safety strategy and disassembly time and used the improved discrete bees algorithm to allocate disassembly tasks. Their safety strategy is to consider the location between human workers and robots. As a human worker approaches the robot, the operation speed of the robot will slow down to avoid robot accidents.

Although previous studies have considered different factors when allocating tasks in human–robot collaboration, no study has considered disassembly cost, disassembleability, and safety to the best of our knowledge. Combining additional attributes and considering the uncertainty are the primary contributions of this study. We propose an optimization-based disassembly sequence planning by considering three attributes, including cost, disassembleability, and safety. The study uses a multi-attribute utility function to combine these attributes. We consider the disassembly time as an uncertain variable with a Beta probability distribution [21]. Besides disassembly cost (time), we also consider disassembleability, which defines the robotic capability on disassembly [18,22], and operator safety, which is modeled by using the strain index (SI) [23]. Table 1 compares this study with previous studies.

The objective of the study is to find the optimal disassembly sequence and allocate disassembly tasks between humans and robots.

The feasible disassembly sequences for a given product can be presented in the form of a graph, as shown in Fig. 1, for a simple product with three components. Each path has different costs, safety, and difficulty.

2 Methodology

This section describes the three attributes incorporated in the objective function and the proposed optimization model based on the concept of a multi-attribute utility function.

2.1 Utility Function. The three attributes include disassembly cost, disassembleability, and safety. The individual utility functions of these three attributes have been integrated to form the overall utility function as shown in Eqs. (1)–(3). $U_{a,j}$ shows the utility function of attribute a for disassembly task j, and k_a is the scaling constant for attribute a. The scaling constant K is determined using Eq. (2). The implementation details can be found in Refs. [24–26]

$$U_{j} = \sum_{j \in J} \frac{1}{K} \left\{ \prod_{a \in A} \left[Kk_{a}U_{a,j} + 1 \right] - 1 \right\}$$
 (1)

$$1 + K = \prod_{a \in A} [Kk_a + 1] \tag{2}$$

$$U_{a,j} = E[U(y)] = \int U(y)f(y)dy$$
 (3)

The scaling constant K is found in Eq. (2). Since some attributes such as disassembly time are uncertain, instead of utility function U(y) the expected utility is used as shown in Eq. (3). For details, see Refs. [24–26].

Each attribute is normalized to unify the unit and range. Also, each attribute is utility independent of other attributes. According to Clemen and Reilly [27], an attribute is a utility independent of another attribute, if preferences for uncertain choices possessing different attribute levels are independent of the values of another attribute. For example, disassembly cost and disassembleability are preferentially independent and utility independent since, regardless of the value of disassembly cost, the user always prefers lower complexity (higher disassembleability) over higher complexity. Even in the case of uncertain choices involving different values

of disassembleability, the user's preference among the uncertain cases is independent of disassembly cost. We should note that the concept of preferential independence and utility independence is separate from how attributes are calculated.

2.2 Disassembly Cost. The disassembly cost depends on the disassembly time which is modeled as an uncertain variable. Fischer et al. [21] showed that the disassembly time could be well described as a Beta distribution

$$\begin{cases} f(t) = \frac{\Gamma(p+q)}{r\Gamma(p)\Gamma(q)} \left(\frac{t-t_L}{r}\right)^{p-1} \left(\frac{t_U-t}{r}\right)^{q-1} & \text{if } t_L \le t \le t_U \\ = 0 & \text{Otherwise} \end{cases}$$
(4)

where
$$r = t_U - t_L$$
 (5)

The t_U and t_L are the range of disassembly time, p, q are shape parameters, and Γ is the gamma function.

We assume exponential functions for cost and time as shown in Eq. (6) since higher time results in more human fatigue, lower performance, and higher opportunity cost. Glock et al. [28] used the exponential function to describe human fatigue, and Potkonjak et al. [29] introduced robot fatigue and used the exponential function for fatigue quantification

$$C_i(t) = de^{ct} (6)$$

where $C_j(t)$ is the disassembly cost of task j with time t; d and c are the constant parameters. The utility function for disassembly cost is as follows:

$$U(C_j) = \frac{C_j(t) - C_{min}}{C_{max} - C_{min}} \tag{7}$$

where
$$C_{max} = de^{ct_{max}}$$
 and $C_{min} = de^{ct_{min}}$ (8)

The utility function of cost is normalized between 0 and 1 using C_{max} and C_{min} as maximum and minimum disassembly costs. Given the uncertainty of disassembly time, the expected cost is described

$$E[U(C_j)] = \int_{t_L}^{t_U} \left(\frac{C_j(t) - C_{min}}{C_{max} - C_{min}}\right) f(t) dt$$

$$= g \int_{t_L}^{t_U} \left(\frac{C_j(t) - C_{min}}{C_{max} - C_{min}}\right) \left(\frac{t - t_L}{r}\right)^{p-1} \left(\frac{t_U - t}{r}\right)^{q-1} dt$$
(9)

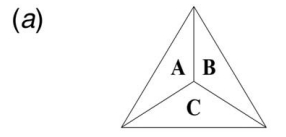
where
$$g = \frac{\Gamma(p+q)}{r\Gamma(p)(q)}$$
 (10)

2.3 Operator Safety. Besides disassembly cost, operator safety is another important attribute. The SI, proposed by Moore and Garg [23], is a well-known tool to evaluate the risk of developing musculoskeletal disorders in distal upper extremities, including the hand, wrist, forearm, and elbow. Given that the e-waste disassembly task requires a lot of upper limb movements, such as disconnecting cables and loosening screws, the SI score is a suitable method to quantify human physical stress in our study. The disassembly tasks are assigned to human and robot based on SI scores to release human physical stress.

The SI score is determined based on the subjective ratings of six task variables, including (1) intensity of exertion (IE), (2) duration of exertion (DE), (3) efforts per minute (EM), (4) hand/wrist posture (HWP), (5) speed of work (SW), and (6) duration per day (DD). A multiplier is then assigned to each task variable based on the ratings. Based on Moore and Garg [23], the rating criteria of the six task variables and their corresponding multipliers are summarized in Tables 2 and 3, respectively. Finally, the SI score is computed by

Table 1 Comparison of existing literature and the current study

Reference	Disassembly cost/time	Safety	Disassembleability	Human-robot collaboration	Multi-attribute utility function
[6]	√				√
[10]	✓				
[13]	\checkmark				
[16]	\checkmark		✓	✓	
[17]	\checkmark	✓		✓	
[18]	\checkmark		✓	✓	
[19]	\checkmark			✓	
[20]	\checkmark	✓		✓	
This study	✓	✓	✓	✓	✓



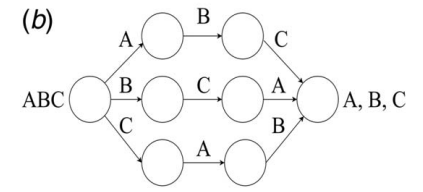


Fig. 1 (a) A simple product with three components and (b) feasible disassembly sequences

Table 2 The rating criterion of the six SI task variables [23]

Rating	IE	DE	EM	HWP	SW	DD
1	Light	<10	<4	Very good	Very slow	≤1
2	Somewhat hard	10–29	4–8	Good	Slow	1-2
3	Hard	30–49	9–14	Fair	Fair	2-4
4	Very hard	50–79	15–19	Bad	Fast	4-8
5	Near maximal	≥80	≥20	Very bad	Very fast	>8

taking the product of the six multipliers

$$SI = IE' \times DE' \times EM' \times HWP' \times SW' \times DD' \tag{11}$$

2.4 Disassembleability. Disassembleability describes the level of complexity of each task. Tasks with high complexity are not feasible to be performed by a robot. The parameters describing disassembleability are introduced in Refs. [18,22] which include: (1) component size (CS), (2) component weight (CW), (3) requirement of tools (T), (4) accessibility (AC), (5) component shape (CSH), (6) operation complexity (OC), (7) positioning (P), and (8) operation force (OF). The scores of each parameter are described in Table 4.

Table 3 The multipliers of the six SI task variables [23]

Rating	IE′	DE'	EM'	HWP'	SW'	DD'
1	1	0.5	0.5	1.0	1.0	0.25
2	3	1.0	1.0	1.0	1.0	0.50
3	6	1.5	1.5	1.5	1.0	0.75
4	9	2.0	2.0	2.0	1.5	1.00
5	13	3.0	3.0	3.0	2.0	1.50

The disassembleability score (DS) is computed by adding up the eight parameters $% \left(\frac{1}{2}\right) =\left(\frac{1}{2}\right) \left(\frac{1}{2}\right$

$$DS = CS + CW + T + AC + CSH + OC + P + OF$$
 (12)

If DS is higher than 14.2 or the robot's capability, the tasks are assigned to the human worker since they exceed the robot's capability [18,22]. The threshold 14.2 is calculated by dividing the summation of the maximum disassembleability of each parameter by 2 e.g., (4+2.4+3+2+1.4+6.5+5+4)/2. The threshold 14.2 is calculated based on the equations provided in Refs. [18,22] and disassembleability parameters are listed in Table 4 for HRC. It should be noted that besides the DS value, other feasibility considerations should be taken into account. For example, if the object is too small or heavy even though the DS is lower than 14.2, the robot still cannot hold and locate the position, therefore the tasks should be assigned to human workers.

2.5 The Proposed Disassembly Sequence Optimization Framework. The multi-attribute utility function U_j shows the overall utility of disassembly operation j, which incorporates the three individual utility functions of cost, disassembleability, and safety. U_j will be used to formulate the objective function of the optimization model. The objective is to maximize the overall utility of the whole sequence. A binary decision variable x_j is defined to determine whether disassembly operation j should be

Table 4 The eight disassembleability parameters [18,22]

CS	Easily grasped Moderately difficult to grasp Difficult to grasp	2 3.5 4
CW	Light Moderately heavy Very heavy	2 2.2 2.4
T	No tools required Common tools required Specialized tools required	1 2 3
AC	Shallow and broad fastener recesses Deep and narrow fastener recesses Very deep and very narrow fastener recesses	1 1.6 2
CSH	Symmetric Semi-symmetric Asymmetric	0.8 1.2 1.4
OC	Low Moderate High	1 4.5 6.5
P	No accuracy required Some accuracy required High accuracy required	1.2 2 5
OF	Low Moderate High	1 2 4

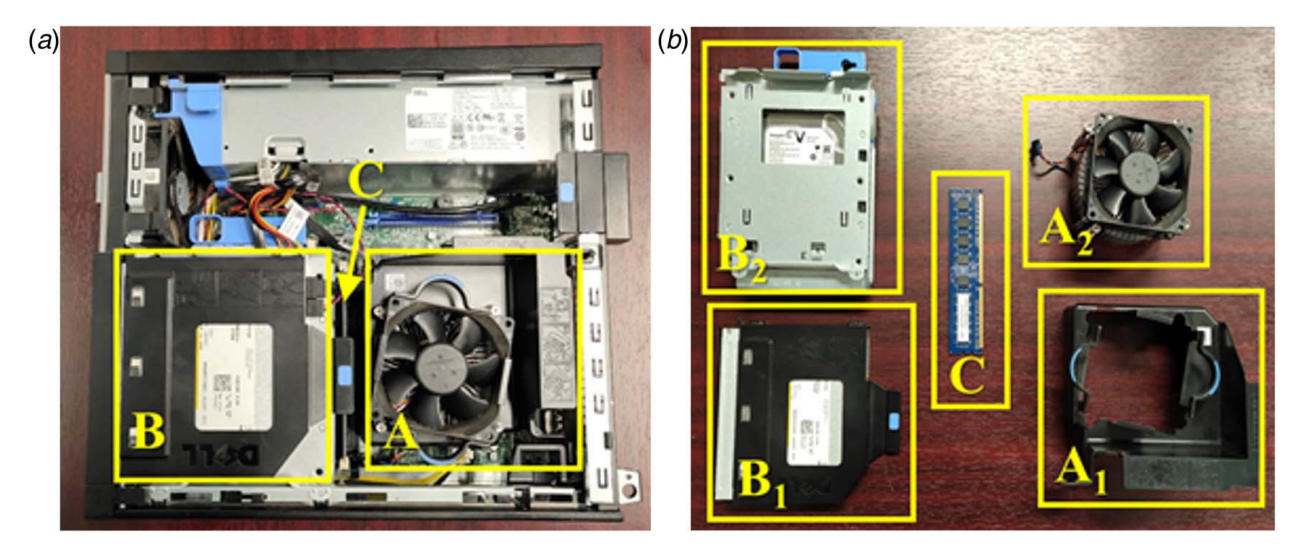


Fig. 2 The desktop components targeted for disassembly

conducted or not. The safety SI scores are used to assign each task to the human worker or robot. Due to the high complexity and uncertainty, tasks with high DS values are given to the human worker. The index set, decision variable, and model parameters are expressed as follows:

Index set	
j	Feasible disassembly transition <i>j</i> (task)
J	The set of all feasible disassembly transitions
a	Attribute <i>a</i>
S	The set of all attributes
M_n	The set of all disassembly transitions going to node n
O_n	The set of all disassembly transitions outgoing from node n
Decision Variables	
x_j	Binary variable $\{0, 1\} = \{\text{not performed, performed}\}$ whether disassembly transition j is performed
α_{j}	Binary variable $\{0, 1\} = \{\text{performed by robot},$
-	performed by human} whether disassembly transition
	j is performed by robot or human
Parameters	
$U_{a,j}$	The single utility function of attribute a for
	transition j
$E[U(C_{R,j})]$	The expected disassembly cost of robot
$E[U(C_{H,j})]$	The expected disassembly cost of human worker
k_a	The scaling constant (a value between 0 and 1)
K	The overall scaling constant (between 0 and 1)
ST, DT	The threshold of SI scores and DS
M	A large enough number. Ex. 10 ¹⁰
y_j	Binary variable {0, 1}

The proposed optimization model for disassembly sequence planning is expressed as

$$Max \sum_{i \in J} \frac{1}{K} \left\{ \prod_{a \in S} [Kk_a U_{a,j} + 1] - 1 \right\} x_j \tag{13}$$

Subject to:

$$U_{1,j} = (1 - \alpha_j) E[U(C_{R,j})] + \alpha_j E[U(C_{H,j})]$$
(14)

$$U_{2,j} = \frac{SI_{max} - SI_j}{SI_{max} - SI_{min}} \tag{15}$$

$$U_{3,j} = \frac{DS_{max} - DS_j}{DS_{max} - DS_{min}} \tag{16}$$

$$(1 - \alpha_i) \cdot (DT - DS_i) \ge 0 \tag{17}$$

$$M(1 - y_i) \ge (DT - DS_i) \tag{18}$$

$$\alpha_i(ST - SI_i) + M \cdot y_i \ge 0 \tag{19}$$

$$\sum_{i \in I} x_j = 1 \text{ (initial node)}$$
 (20)

$$\sum_{i \in M} x_j = \sum_{i \in O} x_j \text{ (transit nodes)}$$
 (21)

$$\sum_{i \in F} x_i = 1 \text{ (target node)}$$
 (22)

$$U_{a,i} \in \{U_{1,i}, U_{2,i}, U_{3,i}\}$$
 (23)

$$0 \le U_{a,j} \le 1 \quad \forall a, \ \forall j \tag{24}$$

Equation (14) shows the expected disassembly cost based on Eq. (9). Equations (15) and (16) reflect the normalization of SI and DS scores for each task between 0 and 1. Equations (17)–(19) are a set of inequalities that represent an if–then statement when solving the task assignment between human and robot. When the task has high safety and disassembleability, it can be assigned to either robot or human; if the expected disassembly cost of the robot is less than the cost of human worker, α_j will be 0. In addition, the SI scores and DS determine α_j based on safety and disassembleability.

3 Case Study: Desktop Disassembly

The data collected from the disassembly of a Dell desktop computer are used as a case study.

Three main components are targeted for disassembly (2a), i.e., component A—heatsink assembly, component B—optical disc drive & hard drive assembly, and component C—memory module. The heatsink assembly, as illustrated in Fig. 2(b), is made up of a fan shroud (A1) and a heat sink (A2), whereas component B consists of an optical disc drive (B1) and a hard drive (B2).

The number of possible disassembly sequences of the three components is six as a permutation problem.

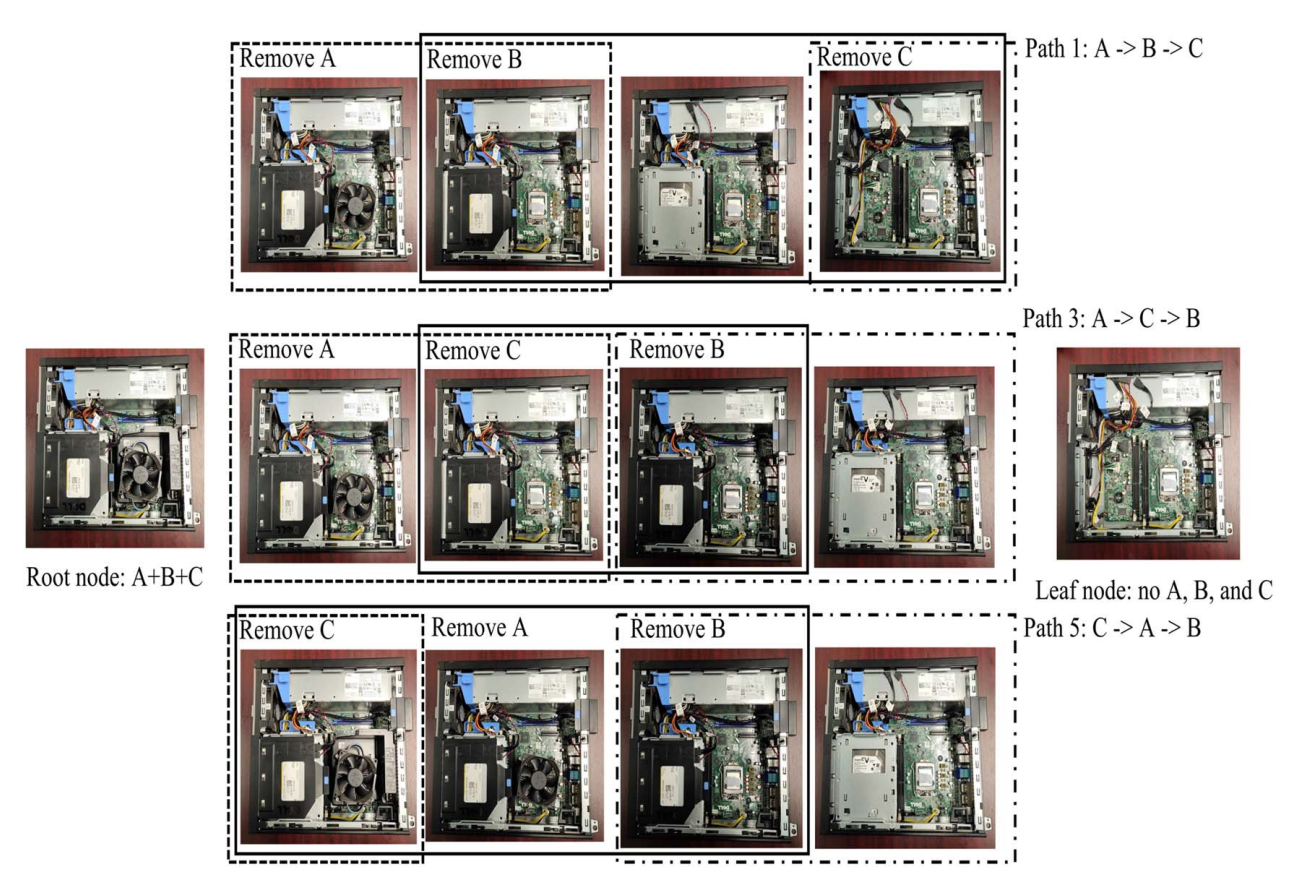


Fig. 3 The three possible disassemble sequences for components A (heatsink assembly), B (optical disc drive and hard drive assembly), and C (memory module)

All six sequences are tested to be feasible in our pilot studies. However, the removal of subassemblies had to be in a specific order due to physical constraints. Specifically, to remove the heat-sink assembly (A) from the computer, the fan shroud (A1) had to be removed before the heat sink (A2) so that cable A2 could be disconnected from the system board. Similarly, to remove component B from the computer, one had to remove the optical disc drive (B1) first to get access to the hard drive (B2). Figure 3 shows the possible disassembly sequences.

To evaluate the SI and DS scores, a participant was tasked with removing the heatsink assembly, the optical disc drive, the hard drive, and the memory module from the desktop computer. Adequate training was given to the participant before the formal data collection. The manufacturer's service manual guided the disassembly procedure. The participant was videotaped during the data collection, performing the disassembly task. After the task was accomplished, the participant was interviewed about their subjective rating of force-related variables, i.e., IE of SI and OF of DS, for every work element. The disassembly of each component is composed of different tasks as shown in Table 5.

Two researchers independently analyzed the video taken during the data collection to obtain the remaining variables. Instead of computing the SI score for the entire job, SI scores for every work task were calculated in the study to validate our optimization model. Furthermore, a default rating value of 4 was assigned to DD, representing a worker performing a given task for 4–8 h [30].

Table 6 shows the disassembly time for human and robot. In this example, the lower bound of disassembly time, t_L for human is determined from experiments. The upper bound of disassembly time for human, t_{IJ} , and disassembly times of robot are assumed.

The disassembly time by the robot is assumed to be greater than human due to the current software and hardware limitations in handling disassembly tasks. The robotic technology for disassembly tasks is not well developed, and most disassembly operations are still conducted manually, so we assume a higher operation time for robots to handle tasks. This may change in the future with more advancements in robotics.

Table 7 summarizes the SI and DS scores for each task. While SI and DS are the same for components A and B removal, the disassembly of component C was highly dependent on the disassembly order of components A and B removal.

As shown in Fig. 2(a), if component C is removed before B and A, the limited space could negatively impact variables such as HWP of SI scores and AC and P of DS. Moreover, poor hand/wrist posture and accessibility made the force exertion difficult, increasing the subjective ratings of IE of SI and DS. Consequently, the SI scores and DS are higher when component C was removed before A and B, performing tasks J16 and J17, and they dropped if A or B was removed before C, performing tasks J12 and J13.

The input parameter d in disassembly cost is assumed to be 5 and 2 for human and robot, respectively, and parameter c is 0.01 in Eq. (6). Due to the limited scope of this study, each disassembly operation is run only once; however, one experiment is not adequate to obtain the exact shape of the distribution function. In practice, comprehensive data collection is needed to empirically gather disassembly time, fit the proper distribution, and estimate the parameters of distribution functions. The relation between disassembly cost and time is plotted in Fig. 4.

The robot costs less than human due to its capability in handling long-term monotonous, repetitive tasks [14,15]. The scaling constants K, k_1 , k_2 , and k_3 are considered as 1.68, 0.17, 0.3, 0.23. The tasks with SI scores higher than 18 are assigned to the robot to reduce musculoskeletal disorders damage to the human worker (Table 7). In this study, normalization is used since each attribute has different ranges and units. Note that k_i are constants in the range of (0, 1). The scaling constants are of the nature of utility

Table 5 The description of disassembly tasks and the corresponding components

Component	Task	Action
Remove Heatsink Assembly (A) (for paths 1–6)	J1	Push away the two release handles while lifting the fan shroud upward and off the computer
	J2	Disconnect the fan cable (with clip) from the system board
	J3 J4	Loosen the captive screws (x4) Lift the heat sink assembly and remove it from the computer
Remove Optical Disc Drive & Hard Drive Assembly (B) (for	J5	Disconnect the data cable from the back of the optical drive
paths 1–6)	J6	Disconnect the power cable from the back of the optical drive
	J7	Lift the tab and slide the optical drive out
	Ј8	Disconnect the data cable from the back of the optical drive
	J9	Disconnect the power cable from the back of the optical drive
	J10	Slide the blue drive cage handle toward the unlocking position
	J11	Lift the hard drive cage from the computer
Remove RAM (C) (For paths 1 & 2, Remove C after removing A and B)	J12	Press down on the memory retaining tabs on each side of the memory module
	J13	Lift the memory module out of the connectors on the system board
Remove RAM (C) (For paths 3 & 4, Remove C between A and B)	J14	Press down on the memory retaining tabs on each side of the memory module
and D)	J15	Lift the memory module out of the connectors on the system board
Remove RAM (C) (For paths 5 & 6, Remove C before removing A and B)	J16	Press down on the memory retaining tabs on each side of the memory module
	J17	Lift the memory module out of the connectors on the system board

Note: The description of disassembly tasks are based on Dell OptiPlex XE2 Small Form Factor Owner's Manual.

Table 6 The upper and lower bounds of disassembly time for human and robot

	Human	worker	Ro	bot
Task	T_L	T_U	T_L	T_U
J1	3	8	4	9
J2	3	8	11	16
J3	53	58	87	92
J4	2	7	3	8
J5	3	8	11	16
J6	3	8	11	16
J7	3	8	4	9
J8	3	8	15	20
J9	3	8	15	20
J10	2	7	3	8
J11	4	9	5	10
J12	3	8	8	13
J13	2	7	3	8
J14	3	8	9	14
J15	2	7	3	8
J16	4	9	16	21
J17	2	7	6	11

Table 7 The results of SI scores and DS for each task

Task	SI scores	DS	Task	SI scores	DS
J1	9	11.2	J10	9	12
J2	18	16.3	J11	18	12
J3	13.5	19.8	J12	9	15.3
J4	9	10	J13	9	10.8
J5	40.5	16.3	J14	13.5	15.9
J6	40.5	16.3	J15	13.5	11.4
J7	9	10.8	J16	54	17.3
J8	54	17.3	J17	18	14.8
J9	54	17.3			

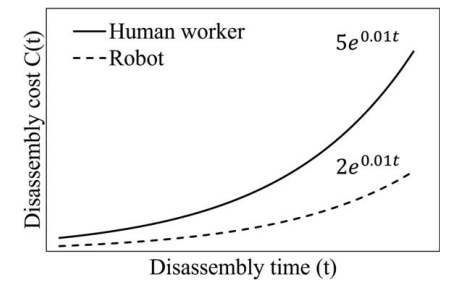


Fig. 4 The disassembly cost of human and robot

where k_i refers to the utility (preference) of an alternative in which the *i*th attribute is at its best level and the rest of the attributes are at their worst levels. For example, 0.3 shows the utility of a disassembly sequence alternative for the decision maker in which the safety is the highest but the cost and disassembly are at their worst levels (highest cost and highest complexity).

4 Results and Discussions

This section shows the optimal sequence and work assignment results. Also, several sensitivity analyses on parameters of the cost function (d and c) have been conducted.

4.1 The Optimal Disassembly Sequence for the Desktop Components. The utility of each attribute and the task assignment among human and robot is shown in Table 8. Some utilities are 0 due to normalization. These tasks reflect either a high SI or high

Table 8 The results of multi-attribute utilities and overall utility for each task (R: robot; H: human worker)

Task	$U_{1,j}$	$U_{2,j}$	$U_{3,j}$	Overall utility U_j	Work assign
J1	0.98	1.00	0.88	0.94	R
J2	0.97	0.80	0.36	0.62	Н
J3	0.08	0.90	0.00	0.29	Н
J4	0.99	1.00	1.00	1.00	R
J5	0.97	0.30	0.36	0.40	Н
J6	0.97	0.30	0.36	0.40	Н
J7	0.98	1.00	0.92	0.96	R
J8	0.97	0.00	0.26	0.24	Н
J9	0.97	0.00	0.26	0.24	Н
J10	0.99	1.00	0.80	0.90	R
J11	0.97	0.80	0.80	0.80	R
J12	0.97	1.00	0.46	0.75	Н
J13	0.99	1.00	0.92	0.96	R
J14	0.97	0.90	0.40	0.68	Н
J15	0.99	0.90	0.86	0.88	R
J16	0.95	0.00	0.26	0.24	Н
J17	0.98	0.80	0.51	0.68	Н

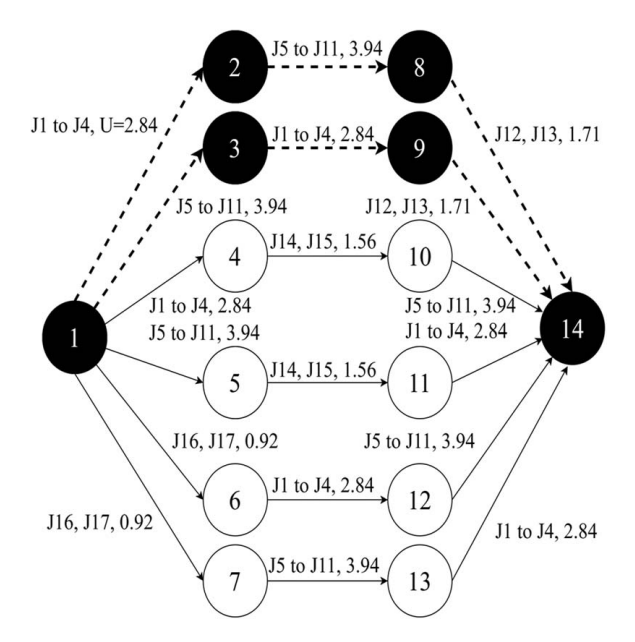


Fig. 5 The summary of feasible and optimal disassembly paths

DS score. For example, $U_{3,j}$ of task J3 equals 0, meaning this task has high values of DS that the robot cannot implement.

J3 is focused on loosening the captive four screws. This task needs high positioning with the small object screws with high complexity and uncertainty. Thus, the task is assigned to the human worker. Some tasks are decided by expected cost when the tasks have low SI scores and high disassembleability. For example, J4 is to lift the heat sink assembly and remove it from the computer with low SI scores and low DS. The task is assigned to robot due to cost-efficiency. Although the robot's disassembly time is higher than that of human worker, the expected disassembly cost of robot is less than the expected cost of human, as discussed in Fig. 4. However, tasks with high SI and DS scores, for example, J9, are assigned to human. Although J9 has a safety issue, it is still assigned to human due to the high operational complexity and infeasibility.

The optimal sequence is shown in Fig. 5. Paths 1–2–8–14 and 1–3–9–14 have the same overall utilities, 8.49, so either path is optimum. Path 1–2–8–14 removes component A before B, and Path 1–3–9–14 removes B before A. Paths 1–4–10–14 and 1–5–11–14 have the same utility, 8.34. Both paths remove component C after A or B. Paths 1–6–12–14 and 1–7–13–14 have the lowest utility of 7.70 since component C is removed first in both paths with limited space.

4.2 Cost Function Sensitivity Analysis. This section describes a sensitivity analysis of the cost function parameters for the robot. Three different combinations of parameters d and c for

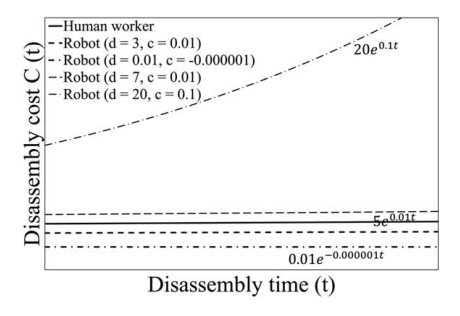


Fig. 6 Condition 1: The robot cost function is either higher or lower than that of the human worker

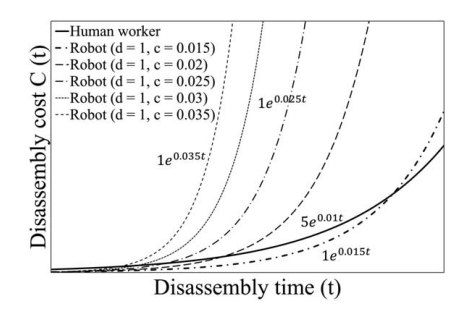


Fig. 7 Condition 2: The robot cost function is lower than the human worker at the beginning and higher at the end

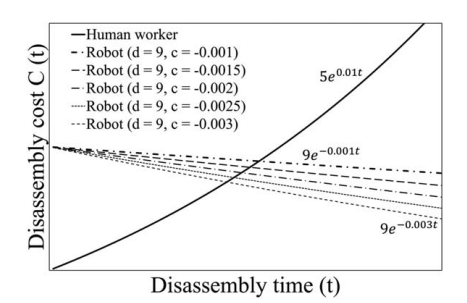


Fig. 8 Condition 3: The robot cost function is greater than human at the beginning and is lower at the end

different conditions are considered. The human cost function is the same as in the previous section, with parameters d=5 and c=0.01. Figures 6–8 show the three different conditions for the robot cost function.

In the first condition, the cost of the robot is either higher or lower than human; in the second condition, the robot's cost is lower at the beginning but will be higher than human as the disassembly time increases. The third condition is the opposite of the second condition.

Table 9 summarizes the results of these three conditions for the work assignments between human and robot. In condition 1, when the parameters change slightly and the robot cost function is close to the human, the results are the same as in the previous section. However, the work assignments will change when the cost function deviates from humans. In condition 2, the work assignments are changed from the human worker to the robot as parameter c increases. In condition 3, the work assignments are switched from robot to human as parameter c decreases.

In practice, the cost function may vary depending on the type of products, robots, and factory configurations. When estimating the cost of operating a robot, various factors such as procurement cost, utilization rate, the efficiency of scheduling, tooling, and setup time should be considered.

4.3 Limitations and Assumptions. The proposed optimization model and the demonstrating case study have several limitations. The operator safety is calculated based on the Strain Index which is focused on the upper extremities. However, disassembly could involve lifting heavy objects which would have an impact on the lower body. Future work should be focused on a diverse set of disassembly tasks that require human movement and lifting of a wide range of objects. More complex case studies on washing machines, printers, and home appliances would enhance the proposed work. Also, another assumption was that a robot can repeatably perform disassembly tasks, however, various factors ranging from environmental conditions to robot degradation and product-to-product variability influence the robot's performance. Future work is needed to incorporate the impact of variable conditions on robot and human performance.

Table 9 The work assignment results of the three sensitivity analysis conditions (R: robot; H: human worker)

Condition 1				Condition 2				Condition 3					
d=3	d = 0.01	d = 7	d = 20	d=1	d = 1	d = 1	d = 1	d=1	d=9	d=9	d=9	d=9	d=9
c =	c =	c =	c =	c =	c =	c =	c =	c =	c =	c =	c =	c =	c =
0.01	-0.000001	0.01	0.1	0.015	0.02	0.025	0.03	0.035	-0.001	-0.0015	-0.002	-0.0025	-0.003
R	R	R	R	R	R	R	R	R	R	R	Н	Н	Н
Н	Н	Н	R	Н	Н	R	R	R	Н	Н	Н	Н	Н
Н	Н	Н	R	Н	R	R	R	R	Н	Н	Н	Н	Н
R	R	R	R	R	R	R	R	R	R	R	R	R	R
Н	Н	Н	R	Н	Н	R	R	R	Н	Н	Н	Н	Н
Н	Н	Н	R	Н	Н	R	R	R	Н	Н	Н	Н	Н
R	R	R	R	R	R	R	R	R	R	R	R	R	Н
Н	Н	Н	R	Н	Н	Н	Н	R	Н	Н	Н	Н	Н
Н	Н	Н	R	Н	Н	Н	Н	R	Н	Н	Н	Н	Н
R	Н	R	R	R	R	R	R	R	Н	Н	Н	Н	Н
R	R	R	R	R	R	R	R	R	Н	Н	Н	Н	Н
Н	Н	Н	R	Н	R	R	R	R	Н	Н	Н	Н	Н
R	R	R	R	R	R	R	R	R	R	Н	Н	Н	Н
Н	Н	Н	R	Н	Н	R	R	R	Н	Н	Н	Н	Н
R	Н	R	R	R	R	R	R	R	Н	Н	Н	Н	Н
Н	Н	Н	R	Н	Н	Н	R	R	Н	Н	Н	Н	Н
Н	Н	Н	R	Н	Н	R	R	R	Н	Н	Н	Н	Н

5 Conclusion

The study proposes an optimization-based disassembly sequence planning framework for human–robot collaboration. It uses the multi-attribute theory to combine three attributes of cost, the complexity of disassembly, and safety to determine the optimal sequence. The disassembly cost is modeled as an uncertain variable with a beta distribution. The safety and disassembleability are modeled using SI and DS scores. The model determines the task assignments among human and robot and determines the optimal disassembly sequence. An example of a desktop computer is used to show the application of the proposed model. In addition, a sensitivity analysis of the robot cost function is discussed.

This study can be extended in several ways. First, the SI scores and DS are currently decided subjectively using standard metrics and conducting lab experiments. However, computer vision techniques can be utilized to quantify the SI scores and DS by observing human and robot disassembly operations. Second, the model can be extended to a real-time sequence planner. Third, other attributes such as the distance between the removal component and the robotic arm position can be further considered in the real-time sequence planner. Fourth, experimental studies can be conducted to provide real disassembly time by robot and the feasibility analysis of each disassembly task.

Acknowledgment

This material is based upon work supported by the National Science Foundation–USA under Grant No #2026276. Any opinions, findings, conclusions, or recommendations expressed in this material are those of the authors and do not necessarily reflect the views of the National Science Foundation.

Conflict of Interest

There are no conflicts of interest.

Data Availability Statement

The datasets generated and supporting the findings of this article are obtainable from the corresponding author upon reasonable request.

Nomenclature

t = disassembly time

 t_U , t_L = upper and lower bounds of disassembly time

 C_{max} = maximum disassembly cost C_{min} = minimum disassembly cost

 U_i = the overall utility of task j

d, c =constant parameters in the disassembly cost function

p, q =shape parameters of the beta distribution

DS = disassembleability scores

SI = strain index scores

 SI_{max} = maximum strain index

 SI_{min} = minimum strain index DS_{max} = maximum disassembleability score

 DS_{min} = minimum disassembleability score

f(y) = the probability density function of attribute y

U(y) = the utility function of attribute y

 $C_i(t)$ = disassembly cost of task j

 Γ = Gamma function

References

- Khatun, A., and Dhara, N., 2022, Smart Cities, Citizen Welfare, and the Implementation of Sustainable Development Goals, A. Pego, ed., IGI Global, Hershey, PA, pp. 222–238.
- [2] Zuidwijk, R., and Krikke, H., 2008, "Strategic Response to EEE Returns: Product Eco-Design or New Recovery Processes?," Eur. J. Oper. Res., 191(3), pp. 1206– 1222.
- [3] Collado-Ruiz, D., and Capuz-Rizo, S. F., 2010, "Modularity and Ease of Disassembly: Study of Electrical and Electronic Equipment," ASME J. Mech. Des., 132(1), p. 014502.
- [4] Ilgin, M. A., and Taşoğlu, G. T., 2016, "Simultaneous Determination of Disassembly Sequence and Disassembly-to-Order Decisions Using Simulation Optimization," ASME J. Manuf. Sci. Eng., 138(10), p. 101012.
- [5] Tao, F., Bi, L., Zuo, Y., and Nee, A. Y. C., 2017, "Partial/Parallel Disassembly Sequence Planning for Complex Products," ASME J. Manuf. Sci. Eng., 140(1), p. 011016.
- [6] Behdad, S., and Thurston, D., 2012, "Disassembly and Reassembly Sequence Planning Tradeoffs Under Uncertainty for Product Maintenance," ASME J. Mech. Des., 134(4), p. 041011.
- [7] Yu, B., Wu, E., Chen, C., Yang, Y., Yao, B. Z., and Lin, Q., 2017, "A General Approach to Optimize Disassembly Sequence Planning Based on Disassembly Network: A Case Study From Automotive Industry," Adv. Prod. Eng. Manage., 12(4), pp. 305–320.
- [8] Bahubalendruni, M. V. A. R., and Varupala, V. P., 2021, "Disassembly Sequence Planning for Safe Disposal of End-of-Life Waste Electric and Electronic Equipment," Natl. Acad. Sci. Lett., 44(3), pp. 243–247.
- [9] Tseng, H.-E., Huang, Y.-M., Chang, C.-C., and Lee, S.-C., 2020, "Disassembly Sequence Planning Using a Flatworm Algorithm," J. Manuf. Syst., 57, pp. 416–428.

- [10] Fu, Y., Zhou, M., Guo, X., Qi, L., and Sedraoui, K., 2021, "Multiverse Optimization Algorithm for Stochastic Biobjective Disassembly Sequence Planning Subject to Operation Failures," IEEE Trans. Syst. Man Cybern. Syst., 52(2), pp. 1041–1051.
- [11] Xia, X., Zhu, H., Zhang, Z., Liu, X., Wang, L., and Cao, J., 2020, "3D-Based Multi-Objective Cooperative Disassembly Sequence Planning Method for Remanufacturing," Int. J. Adv. Manuf. Technol., 106(9), pp. 4611–4622.
- [12] Lee, S.-C., Tseng, H.-E., Chang, C.-C., and Huang, Y.-M., 2020, "Applying Interactive Genetic Algorithms to Disassembly Sequence Planning," Int. J. Precis. Eng. Manuf., 21(4), pp. 663–679.
- [13] Mircheski, I., Pop-Iliev, R., and Kandikjan, T., 2016, "A Method for Improving the Process and Cost of Nondestructive Disassembly," ASME J. Mech. Des., 138(12), p. 121701.
- [14] Li, K., Liu, Q., Xu, W., Liu, J., Zhou, Z., and Feng, H., 2019, "Sequence Planning Considering Human Fatigue for Human–Robot Collaboration in Disassembly," Procedia CIRP, 83, pp. 95–104.
- [15] Vongbunyong, S., Kara, S., and Pagnucco, M., 2013, "Basic Behaviour Control of the Vision-Based Cognitive Robotic Disassembly Automation," Assem. Autom., 33(1), pp. 38–56.
- [16] Xu, W., Tang, Q., Liu, J., Liu, Z., Zhou, Z., and Pham, D. T., 2020, "Disassembly Sequence Planning Using Discrete Bees Algorithm for Human–Robot Collaboration in Remanufacturing," Robot. Comput. Integr. Manuf., 62, p. 101860.
- [17] Lee, M.-L., Behdad, S., Liang, X., and Zheng, M., 2020, "A Real-Time Receding Horizon Sequence Planner for Disassembly in a Human–Robot Collaboration Setting," International Symposium on Flexible Automation, ASME, Paper No. V001T04A004.
- [18] Parsa, S., and Saadat, M., 2021, "Human–Robot Collaboration Disassembly Planning for End-of-Life Product Disassembly Process," Rob. Comput. Integr. Manuf., 71, p. 102170.
- [19] Xu, C., Wei, H., Guo, X., Liu, S., Qi, L., and Zhao, Z., 2020, "Human–Robot Collaboration Multi-objective Disassembly Line Balancing Subject to Task Failure Via Multi-objective Artificial Bee Colony Algorithm," IFAC-PapersOnLine, 53(5), pp. 1–6.

- [20] Xu, W., Cui, J., Liu, B., Liu, J., Yao, B., and Zhou, Z., 2021, "Human–Robot Collaborative Disassembly Line Balancing Considering the Safe Strategy in Remanufacturing," J. Clean. Prod., 324, p. 129158.
- [21] Fischer, J., Stock, P., and Zülch, G., 2005, "Simulation of Disassembly and Re-Assembly Processes With Beta-Distributed Operation Times," *Integrating Human Aspects in Production Management*, G. Zülch, H. S. Jagdev, and P. Stock, eds., Springer, New York, pp. 147–156.
 [22] Parsa, S., and Saadat, M., 2019, "Intelligent Selective Disassembly Planning
- [22] Parsa, S., and Saadat, M., 2019, "Intelligent Selective Disassembly Planning Based on Disassemblability Characteristics of Product Components," Int. J. Adv. Manuf. Technol., 104(5), pp. 1769–1783.
 [23] Steven Moore, J., and Garg, A., 1995, "The Strain Index: A Proposed Method to
- [23] Steven Moore, J., and Garg, A., 1995, "The Strain Index: A Proposed Method to Analyze Jobs for Risk of Distal Upper Extremity Disorders," Am. Ind. Hyg. Assoc. J., 56(5), pp. 443–458.
- [24] Thurston, Deborah L., Lewis, Kemper, Chen, Wei, and Schmidt, Linda, 2006, "Utility Function Fundamentals," *Decision Making in Engineering Design*, K. E. Lewis, W. Chen, and L. C. Schmidt, eds., ASME Press, New York, pp. 15–19.
- [25] Thurston, Deborah, Lewis, Kemper, Chen, Wei, and Schmidt, Linda, 2006, "Multi-Attribute Utility Analysis of Conflicting Preferences," *Decision Making in Engineering Design*, K. E. Lewis, W. Chen, and L. C. Schmidt, eds., ASME Press, New York, pp. 125–133.
- [26] Thurston, D. L., Carnahan, J. V., and Liu, T., 1994, "Optimization of Design Utility," ASME J. Mech. Des., 116(3), pp. 801–808.
- [27] Clemen, R. T., and Reilly, T., 2013, Making Hard Decisions With DecisionTools, Cengage Learning, Mason, OH.
- [28] Glock, C. H., Grosse, E. H., Kim, T., Neumann, W. P., and Sobhani, A., 2019, "An Integrated Cost and Worker Fatigue Evaluation Model of a Packaging Process," Int. J. Prod. Econ., 207, pp. 107–124.
- [29] Potkonjak, V., Petrović, V., Jovanović, K., and Kostić, D., 2013, "Human–Robot Analogy – How Physiology Shapes Human and Robot Motion," ECAL 2013: The Twelfth European Conference on Artificial Life, Sicily, Italy, Sept. 2–6, pp. 136– 143
- [30] Pearce, M., Mutlu, B., Shah, J., and Radwin, R., 2018, "Optimizing Makespan and Ergonomics in Integrating Collaborative Robots Into Manufacturing Processes," IEEE Trans. Autom. Sci. Eng., 15(4), pp. 1772–1784.